



Coupling of synthesis and modification to produce hydrophobic or functionalized nano-silica particles

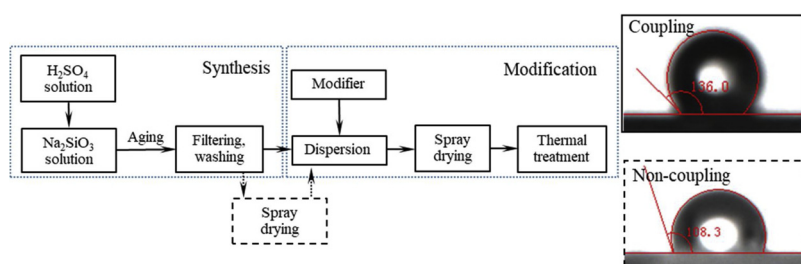
Keyi Yu, Yong Liang, Guanxiang Ma, Ling Yang, Ting-Jie Wang*

Department of Chemical Engineering, Tsinghua University, Beijing, 100084, China



GRAPHICAL ABSTRACT

Coupling of the synthesis and surface modification processes for hydrophobic or functionalized nano-silica particles was performed. Highly hydrophobic and high-density amino-functionalization were achieved for the nano-silica particles via the coupled process using SDS and APTES as modifiers, respectively. The coupled process was proven more effective than the non-coupled process.



ARTICLE INFO

Keywords:
Nano-silica
Modification
Coupling
Hydrophobicity
Functionalization

ABSTRACT

The processes of synthesis and surface modification were coupled herein to produce hydrophobic or functionalized nano-silica particles. Nano-silica particles with a spherical shape approximately 20 nm in diameter were synthesized. Nano-silica particles with high hydrophobicity were produced by coupling the synthesis with a modification process involving aqueous mixing, spray-drying, and thermal treatment, using the common surfactant sodium dodecyl sulfate (SDS) as a modifier. Amino-functionalized nano-silica particles with high grafting density were produced via the same process using the silane coupling agent γ -aminopropyltriethoxysilane (APTES). The modification was more effective with the coupled process than with the non-coupled process.

1. Introduction

Nano-silica particles are widely used in composite materials such as rubbers, resins, pigments, and paints [1–4]. “Green tires” have attracted much attention both in industry and academic research for improving tire performance [5–7]. Nano-silica particles also have specialized application in many other fields such as fillers, catalyst carriers, and biological and medicinal materials, which are required to be modified by functional chemical groups, e.g., amidogens, unsaturated bonds, and mercapto groups [8–12]. Nano-silica particles, especially precipitated

silica, are common products in industry due to their high productivity and low cost of production. However, nano-silica particles have strong polarity due to the abundant hydroxyl groups on particle surface, which makes the particles agglomerate easily, resulting in poor dispersion in the polymer matrix or poor performance in materials [13]. Surface modification plays a key role in the performance of nano-silica particles, and the modified silica with surface functionalization and high grafting ratio are desired.

A modification process is usually conducted in organic solvents for common organic modifiers, such as silane coupling agents, long chain

* Corresponding author.

E-mail address: wangtj@tsinghua.edu.cn (T.-J. Wang).

<https://doi.org/10.1016/j.colsurfa.2019.04.077>

Received 7 March 2019; Received in revised form 20 April 2019; Accepted 25 April 2019

Available online 25 April 2019

0927-7757/ © 2019 Elsevier B.V. All rights reserved.

alcohols [14,15], and alkanolic acids [16–18], because hydrophobic modifiers are easily dispersed in organic solvents. However, the hydrophilic particles still tend to agglomerate in the solvents. Since organic solvents are usually flammable, explosive, and toxic, the recycling, safety, and environmental pollution due to the use of organic solvents must be considered. Hence, this method cannot be productively realized in industry. Modification in the gas phase, e.g., in a fluidized bed, eliminates the requirement of organic solvents, but presents the problem of limited diffusion as the nano-silica particles are in agglomerate states during the modification process, especially for the precipitated silica. It is usually used for fumed silica to match the dry production route [19–24]. An easy and effective process of modification in aqueous phase for precipitated silica is desired to produce high density surface functionalized particles.

Nano-silica particles, especially precipitated silica, easily agglomerate in the drying process. The nearby silanol groups among the particles easily condense through dehydration resulting in a low grafting ratio in the subsequent modification. There have been many studies on in-situ liquid phase modification by adding agents during the generation of particles [25–30]. However, the environment of the particle formation, such as the solution pH, limits the selection of modifiers and grafting ratio. In addition, unreacted agents are removed during desalting and filtering, which causes inefficient agent utilization and difficulty in recycling the organic agent. To modify the nano-silica particles more effectively during wet synthesis, a process for coupling the synthesis and modification was developed in this work. The modification involves the aqueous mixing of silica particles with the modifier, which prevents particle agglomeration and keeps silanol groups reactive before modification; the spray-drying of the slurry, which keeps most of the agents on the particle surface; and the subsequent thermal treatment of the dry powder, which further enhances the grafting reaction [31].

Two water soluble modifiers are chosen to demonstrate the advantages of the process. For surface hydrophobic modification, the common surfactant sodium dodecyl sulfate (SDS) was used as the representation of the alkanolic acid in this work. SDS is soluble in water, and its ester linkage can hydrolyze when heated [32–34]. This produces a hydrophobic surface for particles and improves compatibility between the particles and the organic matrix.

For nano-silica particle functionalization, γ -aminopropyltriethoxysilane (APTES), which is a common silane coupling agent with an amino group on the end, was used as the modifier in this work. Amino-terminated silica particles have a wide range of applications. They are used not only as a filler in plastic and rubber to increase the abrasion resistance, tensile strength, and rheological properties of the composites [35], but also used as a chromatography stationary phase or adsorbent because of their large adsorption capacity and excellent selectivity for specific metal ions, such as Cu^{2+} , Pb^{2+} , and Hg^{2+} [36–39].

2. Experimental

2.1. Reagents

Sodium silicate solution with a modulus (i.e., mole ratio of $\text{SiO}_2/\text{Na}_2\text{O}$) of 2.23 (Beijing Chemical Works, China) was used to prepare the precipitated nano-silica particles. The APTES (Alfa-Aesar, Johnson Matthey Co. USA) used was analytical reagent (AR) grade, with a purity of 98% and density of 0.948 g/cm^3 . SDS (Sinopharm Chemical Reagent Co. Ltd, China) was AR grade. H_2SO_4 (Beijing Chemical Works, China), anhydrous ethanol (Modern Oriental Technology Development Co. Ltd, Beijing, China), $\text{Na}_2\text{SiO}_3 \cdot 9\text{H}_2\text{O}$ (Beijing Chemical Works, China), NaOH (Beijing Chemical Works, China), and $\text{CuSO}_4 \cdot 4.5\text{H}_2\text{O}$ (Beijing Chemical Works, China) were AR grade.

2.2. Synthesis of nano-silica particles

Optimal reaction conditions were established for the synthesis of nano-silica particles, i.e., the concentration of sodium silicate was 8 wt %, the temperature of the water bath was 75°C , and the titration speed of the 2.4 M H_2SO_4 solution was 3 mL/min, which were determined by orthogonal experiments.

In the literature, the H_2SO_4 solution was titrated into a diluted solution of sodium silicate without an aging stage until reaching the final pH of 5 [40–42]. The nano-silica particles underwent a gelation process, which led to difficulty in washing and filtering. An improved acidification process was designed in two steps: (1) When the solution pH decreased to 10, at which point the solution was about to turn to blue gel, the acidification was stopped and the solution was aged for 40 min; (2) the acidification was continued until the pH reached 5.5, followed by aging for 20 min. The nano-silica particles slurry was desalted by washing and filtering for five times with deionized water. The filtered cake with a solid content of approximately 20 wt% was dispersed into deionized water in a conical flask under magnetic stirring. The formed suspension was divided into two parts; one part was directly spray-dried and the obtained powders were labeled as $\text{SiO}_2(\text{sp})$, and the other part underwent a subsequent modification in a wet process.

2.3. Coupled and non-coupled processes

In the process of drying, the nano-silica particles easily agglomerate due to hydrogen-bond interactions and the condensation of abundant hydroxyl groups on the particle surface. Some agglomerates are difficult to disperse into primary nano-silica particles due to chemical bond formation between the particles during hydroxyl condensation. The previous work developed a modification route of aqueous mixing, spray drying and thermal treatment for commercial nano-silica particles. However, the commercial nano-silica particles are already dried, and the agglomerates have been formed in the drying process, which leads to a poor modification.

Therefore, a coupled process combining the synthesis with the three-step modification was designed as follows. After washing and

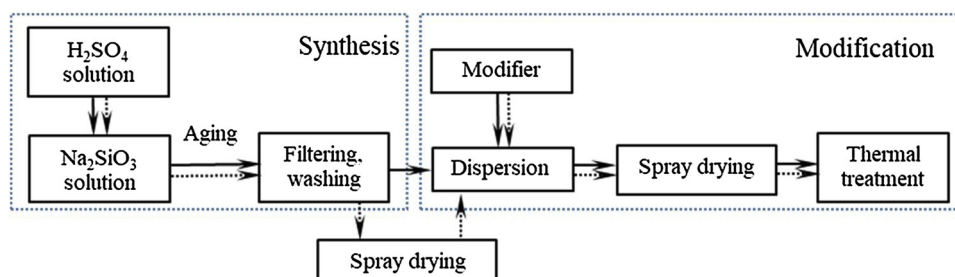


Fig. 1. Coupled (with solid arrow) and non-coupled (with dashed arrow) processes of synthesis and modification for nano-silica particles.

filtering the synthesized nano-silica particles, the modifier was dispersed in the suspension under stirring at room temperature, and then the nano-silica particle suspension was spray-dried and thermally treated. The coupled process is marked by solid arrow in the block diagram in Fig. 1.

Particles synthesized in different methods are quite different in size, morphology and surface hydroxyl properties. In order to make the results comparable, a non-coupled process was designed as follows. The nano-silica particle suspension was directly spray-dried referring to process in the industry, and then dispersed in water, followed by the same modification procedures. The non-coupled process simulated the production process of synthesis first and modification afterward.

2.4. Hydrophobic modification

Modification was conducted with partial reference to our previous work [31,43]. After the suspension of the synthesized nano-silica particles was processed with ultrasonication for 10 min, SDS solution was added. The SDS concentration in the suspension was set to 1.6 wt%, corresponding to the mass ratio of SDS/SiO_2 of 20 wt%. This was designed based on the hydroxyl number on the particle surface of $3\text{--}4\text{ nm}^{-2}$, referring to the literatures' reports [44,45], to ensure that the hydroxyl on the surface of the nano-silica particle was grafted with excess SDS molecules in a mono-layer. For comparison, an experiment with an SDS concentration of 20 wt%, corresponding to a 25 wt% mass ratio of SDS/SiO_2 , was also conducted.

After the addition of SDS, the suspension was stirred for 1 h at room temperature for well mixing. The aqueous mixing was conducted at $pH = 7$ without any organic solvents. The suspension was then dried in a spray-dryer to obtain the dried powders. The air temperatures inlet and outlet were $220\text{ }^\circ\text{C}$ and $80\text{ }^\circ\text{C}$ respectively, and the air flow rate was 40 L/h. The powders were then thermally treated in a sealed steel tube in a muffle furnace at a set temperature of $200\text{ }^\circ\text{C}$ for 30 min according to the optimal conditions in our previous work [31]. After the thermal treatment, the powders were washed with anhydrous ethanol five times to remove the unreacted SDS. Subsequently, the samples were dried at $80\text{ }^\circ\text{C}$ for 24 h. The obtained samples of SDS/SiO_2 20 wt% and 25 wt% were labeled as SiO_2 -SDS-20%-EW and SiO_2 -SDS-25%-EW, respectively.

For comparison, 5 g of spray-dried SiO_2 powders without modification were used to replace the filtered cake of the same mass of SiO_2 , followed with the process as described above, and the sample was labeled as SiO_2 (sp)-SDS-20%-EW.

2.5. High-density silanization with APTES

For modification using APTES, the operational procedure was the same as that described in Section 2.4. The ratio of $APTES/SiO_2$ was set to 1 mL: 1 g, corresponding to the APTES concentration in the suspension of 1.6 wt%.

The nano-silica particle suspension was stirred for 10 min at room temperature for good dispersion without any addition of organic solvents. The mixing time was set to 10 min considering APTES molecules tend to self-condense in water. The pH of the suspension was about 11 due to the alkaline of APTES. The suspension was then dried in a spray-dryer to obtain the dried powders and the spray drying conditions were the same with those in Section 2.4. The powders were then thermally treated at a temperature of $360\text{ }^\circ\text{C}$ for 30 min according to the optimal conditions in our previous work [43]. The obtained sample was labeled as SiO_2 -APTES. The thermally treated particles were thoroughly washed with anhydrous ethanol five times to remove the unreacted APTES. Subsequently, the sample was dried at $80\text{ }^\circ\text{C}$ for 24 h and labeled as SiO_2 -APTES-EW.

For comparison, 5 g of spray-dried SiO_2 powder without modification was used to replace the filtered cake of the same mass of SiO_2 , followed by the procedure described above, and the sample was labeled as SiO_2 (sp)-APTES-EW.

2.6. Characterization

The BET surface area of the nano-silica particles was measured with a surface area analyzer (Autosorb-iQ, Quantachrome Instruments, USA). The crystal structure of the nano-silica particles was inspected using an X-ray diffraction (XRD) analyzer (D8-Advance, Bruker, Germany) at a scan speed of $5^\circ/\text{min}$ over a 2θ range of $10^\circ\text{--}90^\circ$. The morphology of the silica particles was inspected by high-resolution transmission electron microscopy (HRTEM; JEM-2011, JEOL Co., Tokyo, Japan), after the sample was ultrasonically dispersed in ethanol for 10 min. The particle size distribution was measured by dynamic light scattering using Zetasizer (ZS90, Malvern Instruments Ltd, Britain), after the sample was ultrasonically dispersed in ethanol for 30 min. The same sample was repeatedly measured three times and the average was used as the diameter. The contact angle of the sample was measured using a contact angle analyzer (HARKE-SPCA, Beijing Harke, China). The same sample was repeatedly measured five times and the median was used. The characteristic groups on the modified silica surface and modifiers were examined by FTIR spectrometer (Nexus 670, Nicolet, USA) using KBr as the matrix. The grafted amount on the particle surface after ethanol washing was determined by thermogravimetric analysis (TGA; DSC 1, Mettler Toledo, Switzerland). In TGA, the heating rate was set to 20 K/min from $30\text{ }^\circ\text{C}$ to $900\text{ }^\circ\text{C}$ under an atmosphere of nitrogen. The concentrations of copper ions were measured by an inductively coupled plasma atomic emission spectroscopy (ICP-AES; FHM22, SPECTRO, Germany) to determine the adsorption performance of APTES-modified silica. The same sample was repeatedly measured three times and the average was used as the concentration.

2.7. Cu^{2+} adsorption

The Cu^{2+} adsorption performance was used to verify the functionalization of the APTES-modified silica. The concentration of copper ions was measured by ICP-AES with a detection range of $10^{-2}\text{--}10^4$ ppm. The initial concentrations of $CuSO_4\cdot 4.5H_2O$ were set to 100, 200, 400, 800, 1600 and 3200 mg/L, corresponding to the Cu^{2+} concentrations at 25.5, 51.2, 102.4, 204.8, 409.6 and 819.2 mg/L, respectively. 25 mg of APTES-modified particles were added to 50 mL of prepared $CuSO_4$ solutions at different initial concentrations. The suspensions were sufficiently shaken in a constant temperature shaker at $25\text{ }^\circ\text{C}$ for 2 h to reach an adsorption equilibrium. After the adsorption, the solutions were centrifuged, and the Cu^{2+} concentrations of the supernatants were measured by ICP.

3. Results and discussions

3.1. Synthesized nano-silica particles

The synthesized nano-silica particles without a drying process were washed, ultrasonically dispersed in ethanol and sampled to examine the morphology and particle size by TEM. The primary particle size was approximately 20 nm, as shown in Fig. 2. The BET surface area of the nano-silica particles was $302\text{ m}^2/\text{g}$. The specific surface area of ideal spherical particles with a particle size of 20 nm is expected to be approximately $115\text{ m}^2/\text{g}$. The surface area of the synthesized nano-silica particles was about three times of the ideal spherical particles, and also higher than the average value for commercial nano-silica. The larger surface area provides more active hydroxyl to react with modifiers. The crystal structure of the synthesized nano-silica particles was investigated with XRD, as shown in Fig. 3. The nano-silica particles have no characteristic diffraction peak, indicating a typical amorphous structure. The size distributions of particles synthesized with and without spray drying were shown in Fig. 4. The average diameter of the particles synthesized without a drying process is 141.8 nm, and the size distribution is relatively narrow. The drying process increases the average diameter significantly.

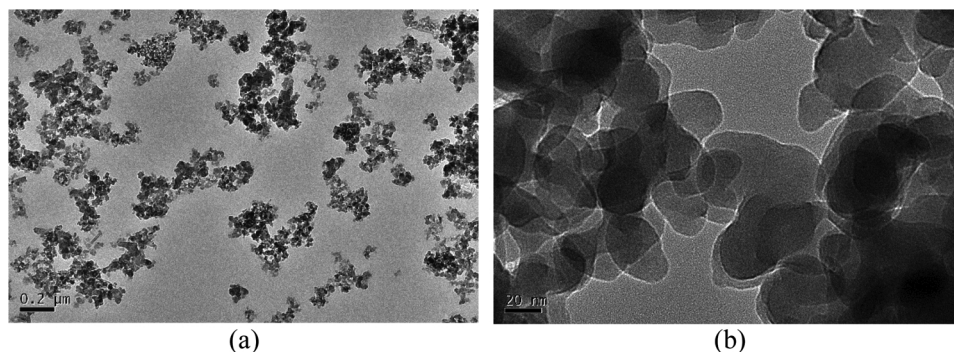


Fig. 2. TEM images of the synthesized nano-silica particles at different amplification times.

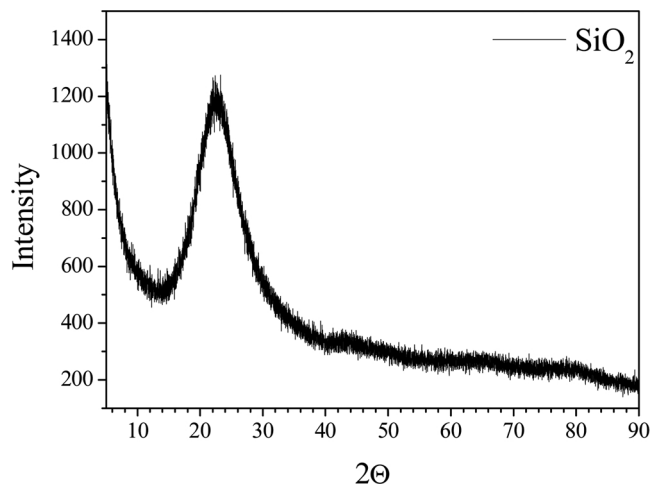


Fig. 3. XRD pattern of the synthesized nano-silica particles.

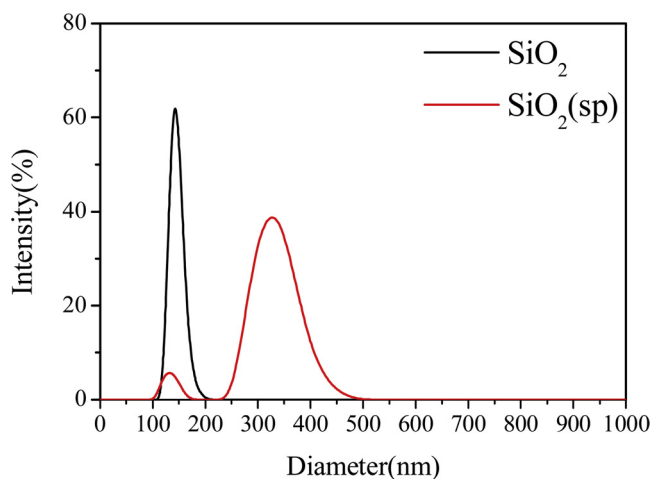
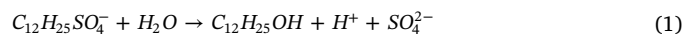


Fig. 4. Size distributions of synthesized nano-silica particles.

3.2. Hydrophobic modification using SDS

3.2.1. Modification process

Modification of the nano-silica particles was conducted successively through aqueous mixing, spray-drying, and thermal treatment. In the aqueous mixing, water-soluble SDS was added into the suspension of the nano-silica particles under stirring, in which the SDS molecules contacted with the silica particles sufficiently. In the spray-drying, SDS physically or chemically adsorbed on the nano-silica particle surface. In the thermal treatment, the unreacted adsorbed-SDS continued to react with the combined water to generate dodecanol as Eq. (1) [32–34],



The dodecanol underwent a dehydration-condensation reaction with the hydroxyl groups on the silica particles, grafting the hydrophobic groups onto the particle surface and converting the particle surface from hydrophilic to hydrophobic. Our previous work had confirmed that SDS and hydroxyl on the silica surface did not undergo a chemical reaction during aqueous mixing or spray-drying. For an effective reaction, the thermal treatment temperature was set to 200 °C [31].

3.2.2. Modification results

The FTIR spectra of SDS-modified samples are measured and the results are shown in Fig. 5. Since the SDS-modified samples have been washed by ethanol for 5 times, the mixed and physically adsorbed SDS is completely removed [31]. The SDS characteristics peaks observed from the SDS-modified sample indicate the SDS is chemically grafted on the particle surface. The small peaks at 2923 cm^{-1} and 2852 cm^{-1} represent $-CH_2$ stretching vibrations, and peaks appearing at 1463 cm^{-1} and 1387 cm^{-1} represent C–H bending vibrations. The asymmetric $-SO_4^{2-}$ stretching vibration appearing at 1025–1210 cm^{-1} can't be observed because of the coincidence of a large peak at 1106 cm^{-1} assigned to the asymmetric Si–O–Si stretching vibration.

To examine the hydrophobicity, the contact angles of the unmodified and modified particles were measured, as shown in Fig. 6. The contact angle of the unmodified particles was only 20°, because the large number of hydroxyl groups made the surface hydrophilic. The contact angle of the modified particles was 136°, which indicated high hydrophobicity of the silica surface.

By analyzing the weight loss of pure SDS as shown in Fig. 7(a), two

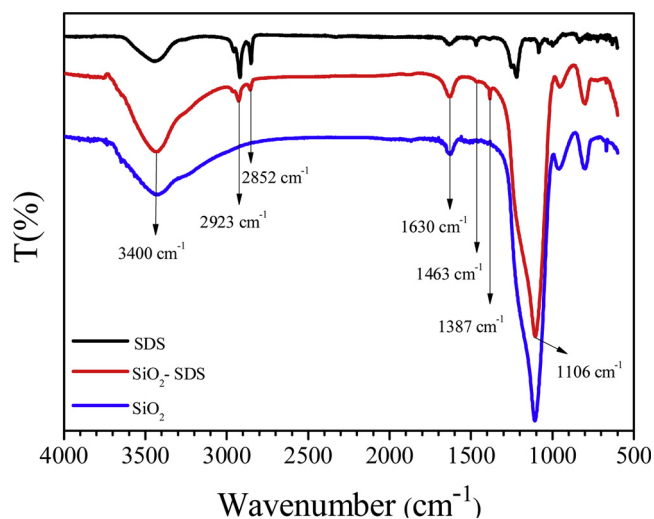


Fig. 5. Infrared spectra of unmodified SiO_2 , pure SDS and SDS modified SiO_2 .

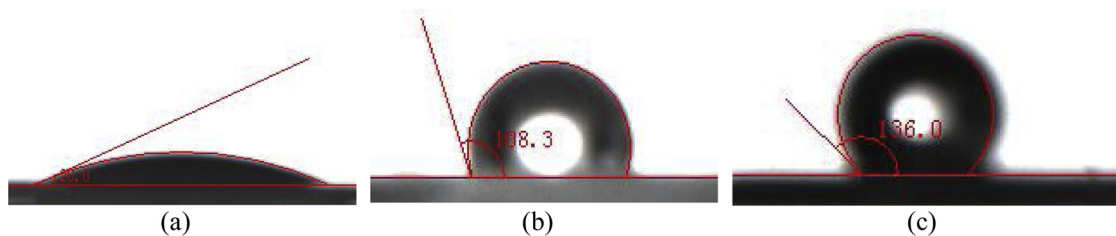
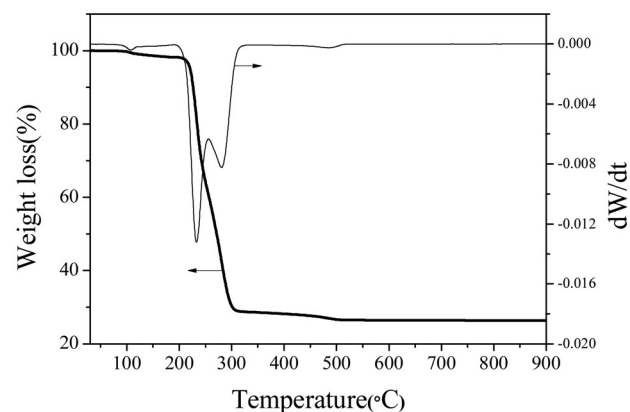
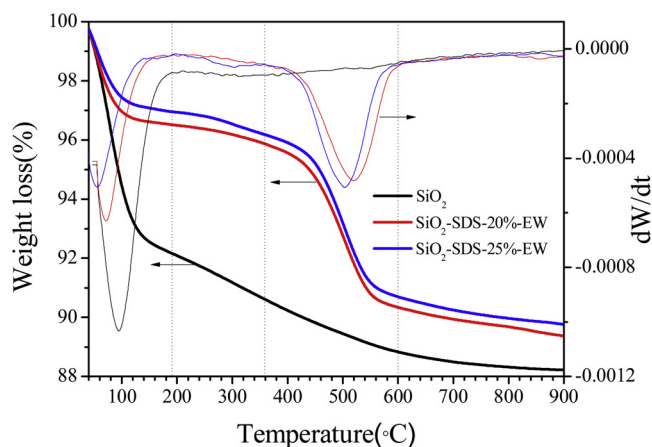


Fig. 6. Contact angles of the unmodified and modified nano-silica particles. (a) unmodified SiO₂ particles, (b) modified SiO₂(sp)-SDS-20%-EW (via the non-coupled process), (c) modified SiO₂-SDS-20%-EW (via the coupled process).



(a)



(b)

Fig. 7. TG curves of (a) pure SDS (b) SDS-modified nano-silica particles at different SDS/SiO₂ ratios.

weight loss peaks at 230 °C and 280 °C were inferred attributing from the evaporation and decomposition of the SDS. By analyzing the weight loss of the modified samples, the amount of SDS grafted onto the particle surface was determined. The TG curves of pure SiO₂, SiO₂ modified with 20 wt% SDS/SiO₂, and SiO₂ modified with 25 wt% SDS/SiO₂ via the coupled process are shown in Fig. 7(b). It is evident that all the samples experience a weight loss in the temperature range of 30–190 °C, which was attributed to the removal of the adsorbed water and part of the hydroxyl on the silica surface [46,47]. The weight loss due to the water on the unmodified particles is much higher than that on the modified particles. This is because the adsorbed SDS occupied active sites on the particle surface and reduced the amount of adsorbed water. As shown in Fig. 7(a), the SDS decomposition finishes at 300 °C, so physically adsorbed SDS doesn't contribute to the weight loss over 300 °C. In the range of 360–600 °C, SiO₂-SDS-20%-EW and SiO₂-SDS-25%-EW show remarkable weight losses, which were attributed to the

decomposition of the SDS grafted onto the silica surface, indicating that SDS was chemically bonded on the silica surface. It is known that the bond energies of Si–O, S–O, C–C, and S–C are 460, 364, 332, and 272 kJ/mol, respectively; thus, the bond energy of C–C is low and the S–C bond is the weakest [48]. This indicates that the decomposition and shedding of C₁₂H₂₅– groups contribute most to the weight loss in the range of 360–600 °C.

In the range of 30–190 °C, the weight loss of SiO₂-SDS-20%-EW is slightly higher than that of SiO₂-SDS-25%-EW. It is inferred that SDS at 20 wt% SDS/SiO₂ occupies fewer active sites of the particle surface, thereby exposing more water or hydroxyl on the particle surface and resulting in greater weight loss. There is little difference in the weight losses of both samples in the range of 360–600 °C, at 5.76% for SiO₂-SDS-20%-EW and 5.48% for SiO₂-SDS-25%-EW. This suggests that the grafting amount did not increase with increasing SDS addition when SDS is more than that required for mono-layer modification under these experimental parameters.

3.2.3. Grafting density of SDS on the particle surface

The mole number of chemical grafted SDS, n_{SDS} (mol), can be calculated from the weight loss in the temperature range of 360–600 °C,

$$n_{SDS} = \frac{\Delta W (\%) \times m_{360}}{M_{C_{12}H_{25}}} \quad (2)$$

where the weight loss (%) at 360–600 °C can be calculated as $\Delta W = (m_{360} - m_{600})/m_{360} \times 100\%$, and $M_{C_{12}H_{25}}$ (g/mol) is the molecular weight of the C₁₂H₂₅ group, i.e., 169 g/mol.

The corresponding surface area S (nm²) of the silica particles is given by,

$$S = (m_{SiO_2} - m_{water}) \times S_{BET-SiO_2} \times 10^{18} \quad (3)$$

where the mass of SiO₂ in the SDS-modified sample is given by $m_{SiO_2} = 1 - n_{SDS} \times M_{C_{12}H_{25}}$, and $S_{BET-SiO_2}$ (m²/g) is the specific surface area of the silica particles, i.e., 302 m²/g, as mentioned above. Then, the number of SDS molecules grafted on the silica surface per square nanometer, n_{SDS}^s (nm⁻²), is calculated as,

$$n_{SDS}^s = \frac{n_{SDS} \times N_A}{S} = \frac{\frac{\Delta W (\%) \times m_{360}}{M_{C_{12}H_{25}}} \times N_A}{(1 - \frac{\Delta W (\%) \times m_{360}}{M_{C_{12}H_{25}}} \times M_{C_{12}H_{25}} - m_{water}) \times S_{BET-SiO_2} \times 10^{18}} \quad (4)$$

3.2.4. Comparison of hydrophobicity modification via the coupled and non-coupled processes

During the coupled process, modifier was added into the suspension of the synthesized nano-silica particles, followed by spray-drying and subsequent thermal treatment. Because the nano-silica particles can achieve excellent dispersion in an aqueous suspension, the coupled process ensures sufficient contact between the nano-silica particles and modifier molecules. In the non-coupled process, the synthesized nano-silica particle suspension was spray-dried, which is the production process most often used in the industry for non-modified nano-silica particles. The dried powders were then dispersed in water with the

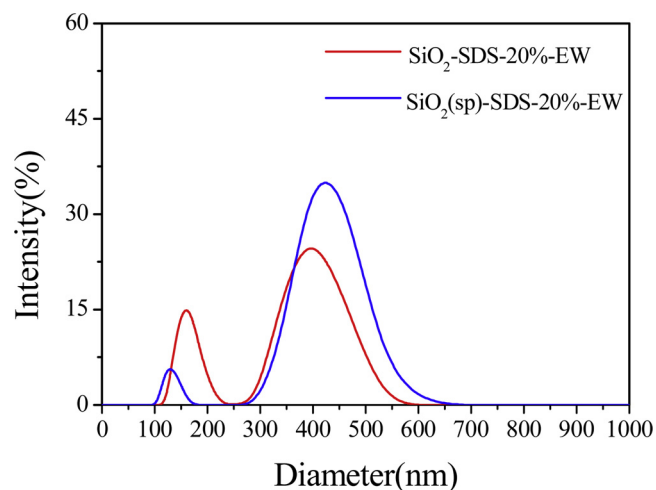


Fig. 8. Size distributions of SDS-modified particles via the coupled and non-coupled processes.

addition of the modifier, followed by the same procedure of spray-drying and subsequent thermal treatment. In practical operation, some of the synthesized nano-silica particles were taken out of the suspension and spray-dried, then followed by the modification in the non-coupled process. For better comparability, all operating conditions in the two processes were kept the same.

The size distributions of particles modified via coupled and non-coupled processes were shown in Fig. 8. The average diameters of particles modified via coupled and non-coupled processes are 331.5 nm and 480.3 nm, respectively. The hydrophobicity of the modified nano-silica particles was measured. For the coupled process, the contact angle of the modified particles is 136°, while for the non-coupled process, the contact angle of the modified particles is 108° in Fig. 6. This shows that the coupled process provides a higher hydrophobicity to the modified particles than the non-coupled process does.

The TG curves of the modified nano-silica particles for the coupled and non-coupled processes are shown in Fig. 9. From Fig. 9, the weight loss of SiO₂-SDS-20%-EW (via the coupled process) in the range of 360–600 °C is 5.76%, while that of SiO₂(sp)-SDS-20%-EW (via the non-coupled process) is 4.12%. The number of SDS molecules grafted on the silica surface per square nanometer, n_{SDS}^s , for SiO₂-SDS-20%-EW was calculated to be 0.72 nm⁻², which is obviously higher than the 0.47 nm⁻² for SiO₂(sp)-SDS-20%-EW, confirming that the modification via the coupled process is more effective than that via the non-coupled process.

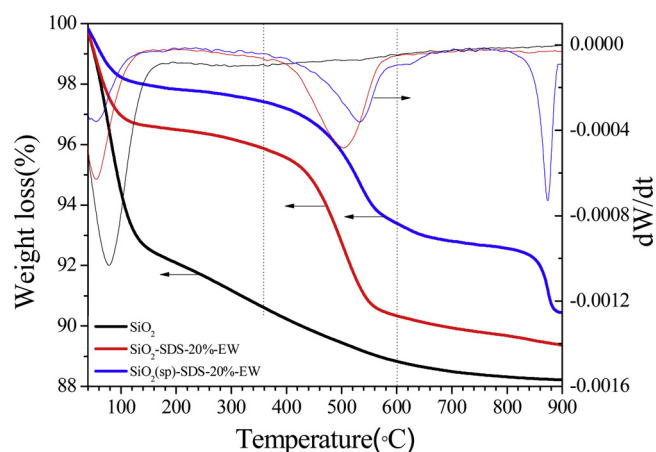


Fig. 9. TG curves of SDS-modified particles via the coupled and non-coupled processes.

Table 1

Modification results via the coupled and non-coupled processes.

Sample	Contact angle (°)	ΔW (%)	n_{SDS}^s (nm ⁻²) (S = 302 m ² /g)	Apparent n_{SDS}^s (nm ⁻²) (S = 115 m ² /g)
SiO ₂ -SDS-20%-EW	136	5.76	0.72	1.89
SiO ₂ (sp)-SDS-20%-EW	108	4.12	0.47	1.23

The excellent modification via the coupled process is attributed to the excellent dispersion of the nano-silica particles in aqueous solution and the sufficient contact of the primary particles with the SDS molecules. Spray-drying before modification in the non-coupled process results in the agglomeration of nano-silica particles, making the dispersion in the primary particles more difficult.

In fact, only the modification on the external surface is effective for the dispersion of nano-silica particles in the organic substrates. For easier understanding, the apparent grafting density was estimated with the assumption that only the external surface of SDS was modified, by using the specific surface area of idea spherical particles with a diameter of 20 nm, i.e., 115 m²/g. With the density of silica assumed to be 2.6 g/cm³, the apparent grafting density, n_{SDS}^s , was calculated, and is shown in Table 1. A high SDS grafting density indicates higher hydrophobicity and better compatibility with nonpolar rubber substrates.

Considering that the addition of SDS is sufficient and the modification is enhanced by the thermal treatment, it is inferred that the grafting density of SDS for SiO₂-SDS-20%-EW is the highest under these experimental parameters.

3.3. High-density silanization using APTES

3.3.1. Silanization process and results

APTES is a typical silane coupling agent. The reaction process of silane coupling agent grafting onto the silica surface can be divided into four steps [49], i.e., (1) the silane coupling agent undergoes hydrolysis; (2) the adjacent hydroxyls of the silane coupling agent form a siloxane oligomer from the condensation reaction; (3) the siloxane oligomer grafts onto the silica surface through a hydrogen bond interaction; (4) a covalent linkage is formed during dehydration via drying or curing. The hydrolyzed APTES reacts on the silica surface with three possible paths, forming a monodentate, bidentate, or tridentate structure, as shown in the schematic diagram of Fig. 10. A higher density of APTES grafting indicates that the surface of the particles was modified with more active amino groups, thereby providing more functionalization sites. Some studies have shown that thermal treatment converts the bonding state of APTES on the nano-silica particle surface from a monodentate into a bidentate or tridentate structure [50–53].

The FTIR spectra of APTES-modified samples were measured and the results are shown in Fig. 11. Since the APTES-modified samples

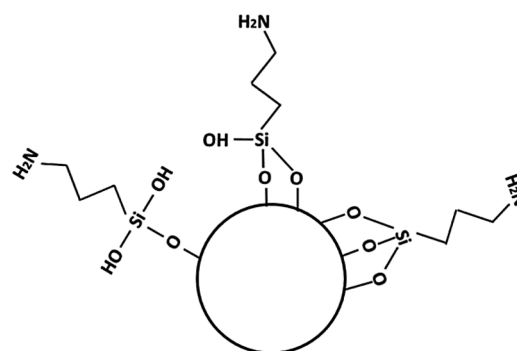


Fig. 10. Schematic diagram of the three bonding paths of APTES on the particle surface.

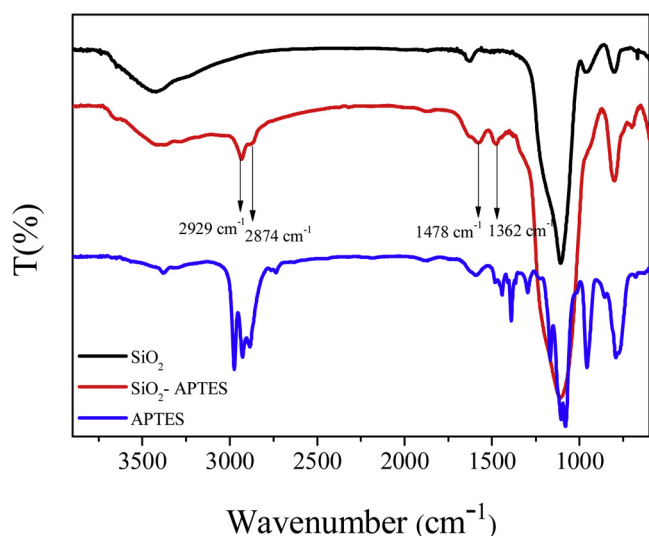


Fig. 11. Infrared spectra of unmodified SiO₂, pure SDS and SDS-modified SiO₂.

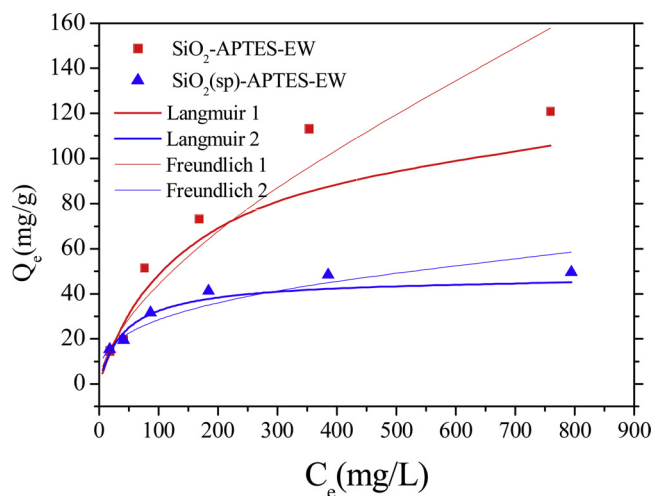


Fig. 12. Cu²⁺ adsorption isotherms of APTES-modified particles and fitting curves.

Table 2

Fitting parameters of the adsorption isotherms of the APTES-modified particles.

Parameters	Langmuir model			Freundlich model		
	$Q_{L, max}$ (mg/g)	b (L/mg)	R^2	K_f (mg/g)	n (L/mg)	R^2
SiO ₂ -APTES-EW	126.58	0.007	0.925	2.60	1.61	0.928
SiO ₂ (sp)-APTES-EW	47.39	0.024	0.928	6.16	2.97	0.932

have been washed by ethanol for 5 times, the mixed and physically adsorbed APTES was completely removed [43]. The APTES characteristics peaks observed from the APTES-modified sample indicate the APTES is chemically grafted on the particle surface. The small peaks at 2929 cm⁻¹ and 2874 cm⁻¹ represent -CH₂ stretching vibrations, and peaks appearing at 1478 cm⁻¹ and 1362 cm⁻¹ represent C-H bending vibrations. The -NH₂ stretching vibration appearing at 3500–3300 cm⁻¹ can't be observed because of the coincidence of a peak at 3400 cm⁻¹ assigned to O-H stretching vibrations from hydroxyl groups on particle surface.

3.3.2. Cu²⁺ adsorption performance

Amino groups have good chelation on many metal ions. Nano-silica

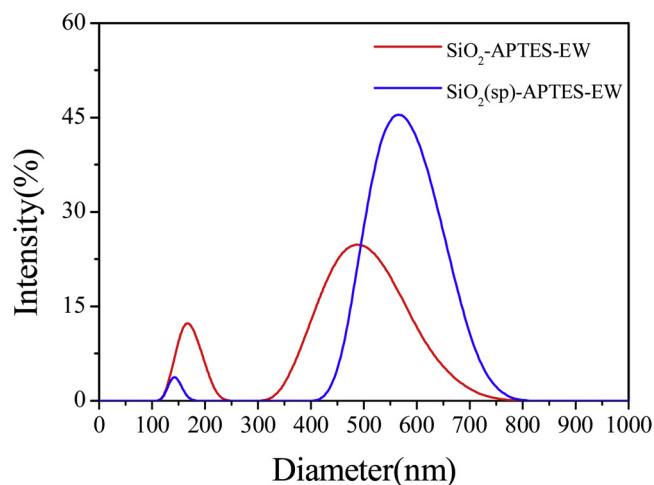


Fig. 13. Size distributions of APTES-modified particles via the coupled and non-coupled processes.

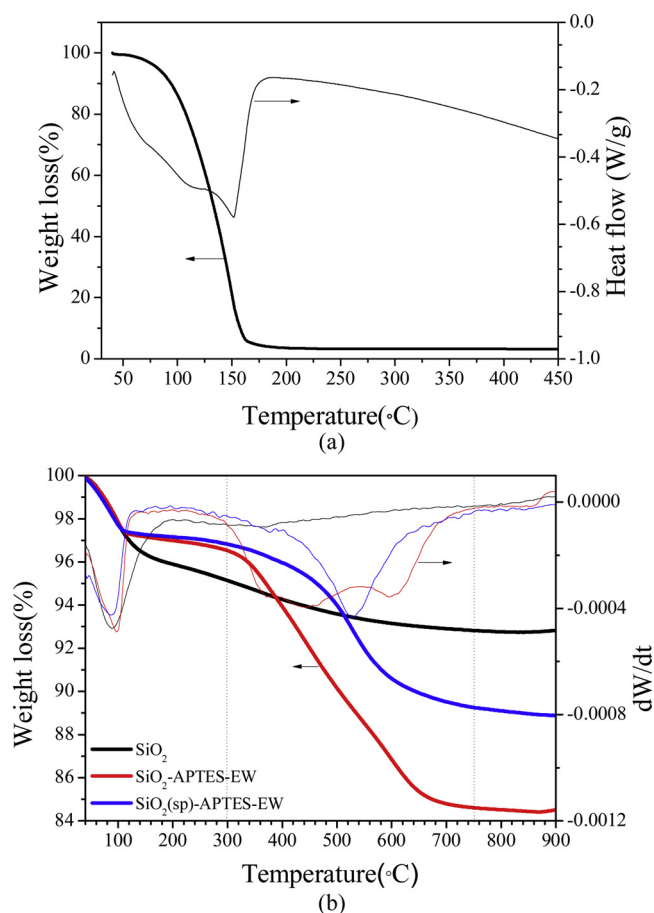


Fig. 14. TG curves of (a) pure APTES (b) APTES-modified samples via the coupled and non-coupled processes.

Table 3

Apparent grafting densities of APTES-modified particles via the coupled and non-coupled processes.

Sample	ΔW (%)	n_A^s (nm ⁻²) ($S = 302$ m ² /g)	Apparent n_A^s (nm ⁻²) ($S = 115$ m ² /g)
SiO ₂ -APTES-EW	12.34	8.55	14.08
SiO ₂ (sp)-APTES-EW	7.81	3.11	8.10

particles functionalized by amino groups have good selectivity and high adsorption capacity for heavy metal ions, such as Cu^{2+} , Pb^{2+} , and Hg^{2+} in water [26,28,29].

The copper adsorption performance of SiO_2 -APTES-EW (via the coupled process) and $\text{SiO}_2(\text{sp})$ -APTES-EW (via the non-coupled process) were examined according to Section 2.7. The adsorption isotherms were measured and fitted with the Langmuir and Freundlich models [54,55], as shown in Fig. 12. The fitting parameters of the adsorption isotherms are given in Table 2. The maximum adsorption capacities $Q_{L, \max}$ of SiO_2 -APTES-EW and $\text{SiO}_2(\text{sp})$ -APTES-EW are 126.58 and 47.39 mg/g, respectively, calculated by the Langmuir model. It indicates that the coupled process is more effective on amino-functionalization than the non-coupled process. The Langmuir model assumes the adsorption to be a homogeneous process. Moreover, the adsorption performance of APTES-modified particles is also well fitted with the Freundlich model, indicating the grafting has the characteristics of multi-layer.

3.3.3. Comparison of silanization via the coupled and non-coupled processes

The size distributions of the particles modified via coupled and non-coupled processes are shown in Fig. 13. The average diameters of particles modified via coupled and non-coupled processes are 468.7 nm and 615.4 nm, respectively. The average diameters of APTES-modified particles are larger than those of SDS-modified particles, due to a certain degree of self-condensation of APTES.

By analyzing the weight loss of pure APTES as shown in Fig. 14(a), the sample has obvious weight loss before 180 °C due to the evaporation, therefore the physically adsorbed APTES doesn't contribute to the weight loss over 180 °C. Fig. 14(b) shows the TG curves of the unmodified particles (SiO_2), the modified particles via the coupled process after ethanol washing (SiO_2 -APTES-EW), and the modified particles via the non-coupled process after ethanol washing ($\text{SiO}_2(\text{sp})$ -APTES-EW). As shown in Fig. 14(b), in the temperature range 300–750 °C, samples SiO_2 -APTES-EW and $\text{SiO}_2(\text{sp})$ -APTES-EW undergo an obvious weight loss, which is attributed to the decomposition of the APTES grafted onto the silica surface, indicating that APTES was chemically bonded on the silica surface. The weight loss of SiO_2 -APTES-EW via the coupled process is 12.34%, and that of $\text{SiO}_2(\text{sp})$ -APTES-EW via the non-coupled process is 7.81%. The weight loss of SiO_2 -APTES-EW is much higher than that of $\text{SiO}_2(\text{sp})$ -APTES-EW, indicating the coupled process was more effective than the non-coupled process for the silanization of nano-silica particles.

Referring to Eqs. (2)–(4), for the silanization of APTES on nano-silica particles, the number of APTES molecules grafted onto the silica surface per square nanometer, n_A^s , can be calculated as Eq. (6),

$$n_A^s = \frac{n_A \times N_A}{S} = \frac{\frac{\Delta W(\%)}{M_{NH}} \times N_A}{\left(1 - \frac{\Delta W(\%)}{M_{NH}}\right) \times M_{A^*} \times S_{BET-SiO_2} \times 10^{18}} \quad (6)$$

The weight loss in the range of 300–750 °C is attributed to the chemically grafted APTES. In Eq. (6), M_{NH} is the molar mass of $\text{NH}_2\text{CH}_2\text{CH}_2\text{CH}_2-$, which is 58 g/mol. The molar masses of grafting groups in the monodentate, bidentate, and tridentate structure are 119, 101, 83 g/mol, respectively. For simplification, the molar mass of the bidentate structure, i.e., 101 g/mol, is used as the average molar mass of grafting groups M_{A^*} . $S_{BET-SiO_2}$ is 302 m^2/g .

The number of APTES molecules grafted onto the silica surface per square nanometer (n_A^s) for SiO_2 -APTES-EW was calculated to be 8.55 nm^{-2} , and is much higher than that for $\text{SiO}_2(\text{sp})$ -APTES-EW of 3.11 nm^{-2} , which also confirms the advantages of the coupled process. For easy understanding and comparison, the apparent grafting density was estimated with the assumption that only the external surface was modified, by using the specific surface area of ideal spherical particles with a diameter of 20 nm, i.e., 115 m^2/g . With the relative density of silica assumed to be 2.6 g/cm^3 , the apparent grafting density (n_A^s) was calculated and is shown in Table 3.

Table 3 shows that the silanization of APTES on the nano-silica particle surface is more effective via the coupled process.

4. Conclusions

Nano-silica particles were synthesized with sodium silicate and sulfuric acid, and modified using SDS and APTES through an aqueous mixing, spray-drying, and thermal treatment process. The synthesis and modification were coupled, and the modification results were compared with that via the non-coupled process. In hydrophobic modification using the common surfactant SDS, the contact angle and the apparent grafting density of the nano-silica particles were 136° and 1.89 nm^{-2} , respectively, via the coupled process, and 108° and 1.23 nm^{-2} via the non-coupled process. During silanization modification, the apparent grafting density reached 14.08 nm^{-2} via the coupled process, and 8.10 nm^{-2} via the non-coupled process. The coupled process was confirmed to be effective, simple, and feasible for the modification of nano-silica particles.

Acknowledgments

The authors wish to express their appreciation for the financial support of this study by the National Key R&D Program of China (2017YED0200704) and the National Natural Science Foundation of China (NSFC No. 21176134).

References

- [1] T. Jesionowski, A. Krysztafkiwicz, Preparation of the Hydrophilic/hydrophobic silica particles, *Colloids Surf. A: Physicochem. Eng. Aspects* 207 (2002) 49–58.
- [2] Y. Li, B. Han, S. Wen, Y. Lu, H. Yang, L. Zhang, L. Liu, Effect of the temperature on surface modification of silica and properties of modified silica filled rubber composites, *Compos. Sci. Technol.* 62 (2014) 52–59.
- [3] S. Kango, S. Kalia, A. Celli, J. Njuguna, Y. Habibi, R. Kumar, Surface modification of inorganic nanoparticles for development of organic-inorganic Nanocomposites-A review, *Prog. Polym. Sci.* 38 (2013) 1232–1261.
- [4] Y. Li, B. Han, L. Liu, Surface modification of silica by two-step method and properties of solution styrene butadiene rubber (SSBR) nanocomposites filled with modified silica, *Compos. Sci. Technol.* 88 (2013) 69–75.
- [5] M. Sakamoto, T. Ono, T. Mafune, Green Tire and Method for Manufacturing Pneumatic Tire, EP, US8028733. (2011).
- [6] H. Li, T. Zhao, M. Chen, Green tire and new type rubber materials, *Chin. Sci. Bull.* 61 (2016) 3297–3303.
- [7] X.B. Zhang, H.Y. Zhang, F.H. Yan, X. Li, T. Ding, Modification of silica and the effect on application of rubber, *Chin. Sci. Bull.* 61 (2016) 3338–3347.
- [8] S. Pausova, J. Krysa, J. Jirkovsky, V. Prevot, G. Mailhot, Preparation of TiO_2 - SiO_2 composite photocatalysts for environmental applications, *J. Chem. Technol. Biotechnol.* 89 (2014) 1129–1135.
- [9] C.J. Galvin, J. Genzer, Applications of surface-grafted macromolecules derived from post-polymerization modification reactions, *Prog. Polym. Sci.* 37 (2012) 871–906.
- [10] E. Reimhult, F. Hook, Design of surface modifications for nanoscale sensor applications, *Sensors* 15 (2015) 1635–1675.
- [11] P. Loganathan, S. Vigneswaran, J. Kandasamy, Enhanced removal of nitrate from water using surface modification of adsorbents - a review, *J. Environ. Manage.* 131 (2013) 363–374.
- [12] S. Prakash, M.B. Karacor, S. Banerjee, Surface modification in microsystems and nanosystems, *Surf. Sci. Rep.* 64 (2009) 233–254.
- [13] X.Y. Ni, J. Sheng, Z.H. Zhang, Physical and chemical properties and applications of nanomaterials, *Chem. Ind. Press.* (2006) 92–93.
- [14] M. Fuji, T. Takei, T. Watanabe, M. Chikazawa, Wettability of fine silica powder surfaces modified with several normal alcohols, *Colloids Surf. A: Physicochem. Eng. Aspects* 154 (1999) 13–24.
- [15] M. Zaboriski, A. Vidal, G. Ligner, H. Balard, Comparative study of the surface hydroxyl groups of fumed and precipitated silicas. I. Grafting and chemical characterization, *Langmuir* 5 (1989) 447–451.
- [16] M. Neouze, U. Schubert, Surface modification and functionalization of metal and metal oxide nanoparticles by organic ligands, *Monatsh. Chem.* 139 (2008) 183–195.
- [17] Z. Hu, Y. Deng, Superhydrophobic surface fabricated from fatty acid-modified precipitated calcium carbonate, *Ind. Eng. Chem. Res.* 49 (2010) 5625–5630.
- [18] X.D. Wu, L.J. Zheng, D. Wu, Fabrication of superhydrophobic surfaces from microstructured ZnO-based surfaces via a wet-chemical route, *Langmuir* 21 (2005) 2665–2667.
- [19] M. Lazghab, K. Saleh, P. Guigon, A new solventless process to hydrophobize silica powders in fluidized beds, *AIChE J.* 54 (2008) 897–908.
- [20] S. Ek, E.I. Iiskola, L. Niinisto, Gas-phase deposition of aminopropylalkoxysilanes on porous silica, *Langmuir* 19 (2003) 3461–3471.
- [21] Z.L. Wang, M. Kwak, H.Z. Li, Fluidization of fine particles, *Chem. Eng. Sci.* 53

- (1998) 377–395.
- [22] D. Geldart, Types of gas fluidization, *Powder Technol.* 7 (1973) 285–292.
- [23] J.R. van Ommen, J. Manuel Valverde, R. Pfeffer, Fluidization of nanopowders: a review, *J. Nanopart. Res.* 14 (2012) 1–29.
- [24] J.L.H. Chau, C. Yang, Surface modification of silica nanopowders in microwave plasma, *J. Exp. Nanosci.* 9 (2014) 357–361.
- [25] S. Poompradub, B. Chaichua, C. Kanchanaamporn, T. Boosalee, P. Prasassarakich, Synthesis of silica in natural rubber solution via sol-gel reaction, *Kgk-Kaut G ummi Kunst.* 61 (2008) 152–155.
- [26] S. Kohjiya, Y. Ikeda, In situ formation of particulate silica in natural rubber matrix by the sol-gel reaction, *J. Sol-Gel Sci. Technol.* 26 (2003) 495–498.
- [27] B. Chaichua, P. Prasassarakich, S. Poompradub, In situ silica reinforcement of natural rubber by sol-gel process via rubber solution, *J. Sol-Gel Sci. Technol.* 52 (2009) 219–227.
- [28] A.S. Hashim, S. Kohjiya, Y. Ikeda, Moisture cure and in-situ silica reinforcement of epoxidized natural rubber, *Polym. Int.* 38 (1995) 111–117.
- [29] N. Watcharakul, S. Poompradub, P. Prasassarakich, In situ silica reinforcement of methyl methacrylate grafted natural rubber by sol-gel process, *J. Sol-Gel Sci. Technol.* 58 (2011) 407–418.
- [30] S. Kohjiya, Y. Ikeda, Reinforcement of natural rubber by silica generated in situ, *Proc. Jpn. Acad. B-Phys.* 76 (2000) 29–34.
- [31] B. Qiao, Y. Liang, T.J. Wang, Y.P. Jiang, Surface modification to produce hydrophobic nano-silica particles using sodium dodecyl sulfate as a modifier, *Appl. Surf. Sci.* 364 (2016) 103–109.
- [32] C.L. Lee, C.C. Wan, Y.Y. Wang, Synthesis of metal nanoparticles via self-regulated reduction by an alcohol surfactant, *Adv. Funct. Mater.* 11 (2001) 344–347.
- [33] Z. Liu, K. Xu, H. Sun, S. Yin, One-step synthesis of single-layer MnO₂ nanosheets with multi-role sodium dodecyl sulfate for high-performance pseudocapacitors, *Small* 11 (2015) 2182–2191.
- [34] C.C. Yang, C.C. Wan, Y.Y. Wang, Synthesis of Ag/Pd nanoparticles via reactive micelles as templates and its application to electroless copper deposition, *J. Colloid Interf. Sci.* 279 (2004) 433–439.
- [35] E.P. Plueddemann, Chemistry of silane coupling agents, *Silane Coupling Agents* (1991) 31–54.
- [36] J.E. O'Gara, D.P. Walsh, C.H. Phoebe, B.A. Alden, Embedded-polar-group bonded phases for high performance liquid chromatography, *LC GC N. Am.* 19 (2001) 632–642.
- [37] E.F. Vansant, P.V.D. Voort, K.C. Vrancken, *Characterization and Chemical Modification of the Silica Surface*, Elsevier, 1995.
- [38] M. Etienne, A. Walcarius, Analytical investigation of the chemical reactivity and stability of aminopropyl-grafted silica in aqueous medium, *Talanta* 59 (2003) 1173–1188.
- [39] H. Wang, L. Yan, R. Zhao, J. Sui, Study on the synthesis and catalytic performance of aminopropyl functionalized SBA-15 mesoporous molecular sieves, *J. Mol. Catal. (China)*. 19 (2005) 1–6.
- [40] C. Zhao, Z. Li, H. Hu, Y. Yang, Y. Huang, J. Yang, In-situ preparation of surface-functionalized SiO₂ nanoparticles with controllable sizes, *J. Nanosci. Nanotechnol.* 17 (2017) 729–734.
- [41] W. Lin, Y. Xu, X. Gong, Study on in-situ preparation of modified silica, *Non-metallic Mines* 36 (2013) 53–54 67.
- [42] D. Li, F. Wang, H. Zhu, Preparation of ultrafine silica nanoparticles by a precipitation method, *J. Beijing Univ. Chem. Technol. Nat. Sci. Ed.* 43 (2016) 33–39.
- [43] B. Qiao, T.J. Wang, H. Gao, Y. Jin, High density silanization of nano-silica particles using γ -aminopropyltriethoxysilane (APTES), *Appl. Surf. Sci.* 351 (2015) 646–654.
- [44] L.T. Zhuravlev, The surface chemistry of amorphous silica: Zhuravlev model, *Colloids Surf. A: Physicochem. Eng. Aspects* 173 (2000) 1–38.
- [45] H. Tamura, A. Tanaka, K. Mita, R. Furuichi, Surface hydroxyl site densities on metal oxides as a measure for the ion-exchange capacity, *J. Colloid Interface Sci.* 209 (1999) 225–231.
- [46] V. Dugas, Y. Chevalier, Surface hydroxylation and silane grafting on fumed and thermal silica, *J. Colloid Interface Sci.* 264 (2003) 354–361.
- [47] V. Dugas, Y. Chevalier, Chemical reactions in dense monolayers: in situ thermal cleavage of grafted esters for preparation of solid surfaces functionalized with carboxylic acids, *Langmuir* 27 (2011) 14188–14200.
- [48] R.A. Howald, *Chemical Bonds and Bond Energy* (Sanderson, R.T.), Academic Press, 1976, p. 1044.
- [49] B. Arkles, Tailoring surfaces with silanes, *Chemtech.* 7 (1977) 766–778.
- [50] E.T. Vandenberg, L. Bertilsson, B. Liedberg, K. Uvdal, R. Eerlandsson, Structure of 3-aminopropyl triethoxy silane on silicon-oxide, *J. Colloid Interface Sci.* 147 (1991) 103–118.
- [51] F.X. Zhang, M.P. Srinivasan, Self-assembled molecular films of Aminosilanes and their immobilization capacities, *Langmuir* 20 (2004) 2309–2314.
- [52] J. Kim, G.J. Holinga, G.A. Somorjai, Curing induced structural reorganization and enhanced reactivity of amino-terminated organic thin films on solid substrates: observations of two types of chemically and structurally unique amino groups on the surface, *Langmuir* 27 (2011) 5171–5175.
- [53] J.H. Moon, J.W. Shin, S.Y. Kim, J.W. Park, Formation of uniform aminosilane thin layers: an imine formation to measure relative surface density of the amine group, *Langmuir* 12 (1996) 4621–4624.
- [54] C. Zhang, Y.Z. Li, T.J. Wang, Y.P. Jiang, J. Fok, Synthesis and properties of a high-capacity Iron oxide adsorbent for fluoride removal from drinking water, *Appl. Surf. Sci.* 425 (2017) 272–281.
- [55] L. Chen, B.Y. He, S. He, T.J. Wang, Fe-Ti oxide nano-adsorbent synthesized by Co-precipitation for fluoride removal from drinking water and its adsorption mechanism, *Powder Technol.* 227 (1) (2012) 3–8.